Journal of Functional Foods 61 (2019) 103487

Contents lists available at ScienceDirect

Journal of Functional Foods

journal homepage: www.elsevier.com/locate/jff

A highly absorbable peptide GLPY derived from elastin protect fibroblasts against UV damage *via* suppressing Ca^{2+} influx and ameliorating the loss of collagen and elastin

Yang Liu[a,b], Guowan Su[a,b], Shuguang Wang[a,b], Baoguo Sun[c], Lin Zheng[a,*], Mouming Zhao[a,b,c,*]

[a] School of Food Science and Engineering, South China University of Technology, Guangzhou 510640, China
[b] Guangdong Food Green Processing and Nutrition Regulation Technologies Research Center, Guangzhou 510650, China
[c] Beijing Advanced Innovation Center for Food Nutrition and Human Health, Beijing Technology & Business University, Beijing 100048, China

ARTICLE INFO

Keywords:
Anti-photoaging
Fibroblasts
MMP-1 and MMP-12
Elastin and collagen mRNA
Simulated gastrointestinal digestion
Digestion and absorption

ABSTRACT

Our previous study showed that elastin hydrolysates could ameliorate UV damage in mice skin and two peptides GLPY and GPGGVGAL with protective effects against UV damage on fibroblast were identified. The aim of this study was to elucidate the underling mechanism. Results showed that GLPY and GPGGVGAL could protect fibroblast from UV damage by suppressing ROS production. Notably, GPGGVGAL could inhibit Ca^{2+} influx more effectively, whereas GLPY displayed stronger suppression on the loss of elastin and collagen type-I, which could result from that GLPY could regulate the mRNA expression of collagen type-I and the level of MMP-12 more efficiently. Additionally, GLPY maintained intact in gastrointestinal tract and could be transferred across Caco-2 monolayers *via* the intracellular transcytosis pathway, whereas GPGGVGAL was completely hydrolyzed by digestive enzymes. Results suggested that GLPY could be potential ingredients used to prevent and regulate the skin photoaging.

1. Introduction

Photoaging of skin induced by UV irradiation is a complex biological process, which is manifested by epidermis hyperplasia, transepidermal water loss and degradation of the extracellular matrix (ECM) (Helfrich, Sachs, & Voorhees, 2008). Elastin and collagen play essential roles in the ECM which provide skin with tensile strength, elasticity and hydration. However, excessive UV exposure could cause an extreme increase of reactive oxygen species (ROS) which is the major factor for photoaging (Muller, Lustgarten, Youngmok, Arlan, & Holly, 2007). High level of ROS is related to the cell damage through multiple pathways, including promoting Ca^{2+} influx (Zhang et al., 2015), inhibiting the synthesis of collagen by activating MAPK pathway (Schwartz, Cruickshank, Christensen, Perlish, & Lebwohl, 2010) and upregulating expression of matrix metalloproteinases (MMPs) (e.g. MMP-1, -2, -3, -7, -9, and -12) (Fisher et al., 2000). MMPs are members of ubiquitous endopeptidases playing a role in degradation of the ECM. Especially, MMP-1 and MMP-12 are the major enzymes to digest collagen and elastin, respectively.

Oxidative stress, loss of collagen and enhancement of MMPs in UV damaged skin have received substantial attention by researchers. It is widely reported that some plant extracts (Kim, 2016; Park et al., 2017) and bioactive peptides (Kwon et al., 2016; Sun, Liu, Fan, Li, & Zhuang, 2018; Ryu, Qian, & Kim, 2010) had reverse effects on UV-induced photodamage through inhibiting the up-regulation of MMPs expression and down-regulation of collagen generation. Hong et al. pointed out that lipoteichoic acid isolated from *Lactobacillus plantarum* could inhibit MMP-1 expression and up-regulates type I procollagen by suppressing the generation of ROS. Sun et al. (2018) also reported that peptides GYTGL, LGATGL, and VLGL could inhibit MMP-1 activity and intercellular ROS production, and the C terminate Gly-Leu of these three peptides played important roles in MMP-1 inhibitory activity. It could be found that researchers mainly focused on the changes in collagenase (e.g. MMP-1) and collagen induced by UV irradiation. However, the influence of UV on elastase (i.e., MMP-12) and elastin, which also play crucial roles in skin aging, were rarely reported. In our previous study (Liu et al., 2018), we elucidated the anti-photoaging effect of bovine elastin hydrolysates on aging skin of mice and also identified two elastase inhibitory peptides, i.e., GLPY and GPGGVGAL, which were proved to improve cell viability of UV-damaged fibroblast. Hence, it is worthy to further investigate the underlying mechanism of the anti-photoaging effects showed by GLPY and GPGGVGAL in fibroblast,

* Corresponding authors at: School of Food Science and Engineering, South China University of Technology, Guangzhou 510640, China (M. Zhao).
E-mail addresses: felinzheng@scut.edu.cn (L. Zheng), femmzhao@scut.edu.cn (M. Zhao).

https://doi.org/10.1016/j.jff.2019.103487
Received 15 December 2018; Received in revised form 1 July 2019; Accepted 30 July 2019

including the oxidative stress, collagenolysis and particularly elastolysis.

Additionally, digestion in gastrointestinal (GI) tract and transepithelial transport across the intestine are the two crucial barriers for oral administration of bioactive nutrients (Wang, Wang, & Li, 2016). Peptides might be further hydrolyzed by pepsin and pancreatin. As Ruiz, Ramos, and Recio (2004) proposed that KKYNVPQL isolated from Manchego cheese was further hydrolyzed while LEIVPK and LPY remained intact during simulated GI digestion. Further, degradation of peptides caused by enzymes in intestinal epithelial cell and the difficult absorption in GI tract might also lead to changes in bioactivity and/or structure of peptides (Lacroix, Chen, Kitts, & Li-Chan, 2017; Wang et al., 2016). Fortunately, dipeptides, tripeptides and some large peptides were proved to maintain the original structure across the Caco-2 cell monolayers (Xu et al., 2017; Yang et al., 2017). Therefore, it is necessary to explore the fate of peptides in gastrointestinal (GI) tract by using simulated GI digestion and Caco-2 cell model *in vitro*.

Therefore, the aim of this study was to further elucidate the protective mechanism of GLPY and GPGGVGAL on UV damaged fibroblasts by measuring ROS generation, Ca^{2+} influx, elastin and collagen type-I concentration, MMPs concentration, and mRNA expression of elastin and collagen. Finally, simulated GI digestion and Caco-2 cell monolayers were used to explore the digestion and absorption of the two peptides.

2. Materials and methods

2.1. Materials and chemicals

Pepsin (40,000 U/g) and pancreatin (240,000 U/g) were obtained from Guangzhou Geneshun Biotech Ltd (Guangzhou, China). Peptides GLPY and GPGGVGAL were chemically synthesized by GL Biochem Ltd. The human foreskin fibroblast (HFF) cell line and Caco-2 cell line were purchased from the Cell Bank of the Chinese Academy of Sciences (Shanghai, China). Reactive oxygen species (ROS) detection kit, superoxide dismutase (SOD) detection kit, mitochondrial membrane potential (MMP) detection kit, Trizol kit and Fura-2 AM were purchased from Beyotime Institute of Biotechnology (Shanghai, China). ELISA kits (for Human Elastin, Collagen type-I, MMP-1, Elastase) were purchased from Jiangsu Meibiao Biotechnology Co Ltd (Yancheng, China). SYBR® Premix Ex Taq™ was obtained from Takara Biomedical Technology Co., Ltd (Beijing, China). All of the solvents for UPLC were of HPLC grade. Other reagents were of analytical grade.

2.2. Fibroblasts cell culture and treatments

The human foreskin fibroblast (HFF) was cultured in Dulbecco's modified Eagle's medium (DMEM) supplemented with penicillin (400 U/ml), streptomycin (50 mg/ml), and 14% fetal bovine serum (FBS) at 37 °C in a humidified atmosphere of 5% CO_2. Cells seeded in 96-well plates (1×10^5 cells/well) were washed with phosphate buffered saline (PBS) and then irradiated with UV treatment (5 J/cm^2). After UV treatment, the culture medium was replaced with fresh medium without FBS but containing 200 μM GLPY or GPGGVGAL, and then the HFF was incubated for 24 h in a humidified atmosphere.

2.3. Determination of SOD, collagen type-I, elastin, collagenase (MMP-1) and elastase (MMP-12) levels

After the cell treatment, the DMEM medium containing synthetic peptide was discarded and then the cells were washed with PBS. The cells digested by 0.25% trypsin were collected and centrifuged at 1000*g* for 3 min (Medifuge™ centrifuge, Thermo Fisher Scientific, USA), and then resuspended in PBS (200 μL) after discarding the supernatant. Then the cells were mixed with 200 μL of RIPA lysate to lyse the cells, and the mixture was centrifuged at 13,000*g* for 5 min at 4 °C. The supernatant was collected and used to measure the SOD, collagen type-I, elastin, MMP-1and MMP-12 levels according to the relevant kit instructions.

2.4. Measurement of intracellular ROS

DCFH-DA fluorescent probe staining is used to measure the intracellular reactive oxygen species. After treating with DMEM containing synthetic peptide for 24 h, the HFF cells were incubated with 10 μM DCFH-DA in a CO_2 incubator (5% CO_2, 37 °C) for 30 min, and then washed with PBS to remove the residual probe. The intensity of fluorescent (Ex = 854 nm, Em = 525 nm) was measured using a microplate reader (Thermo Fisher Scientific, USA).

2.5. Measurement of intracellular calcium concentration of ($[Ca^{2+}]_i$)

At the end of treatment, the cells were digested and centrifuged (1000*g*, 3 min), and then incubated with the Fura-2 probe at 37 °C for 45 min in the dark. After incubation, the cells were washed with PBS and plated on 96-well assay plates. Then the fluorescence intensity at an emission wavelength of 510 nm and excitation wavelength of 340 nm and 380 nm was measured to get the ratio (F_{340}/F_{380}).

2.6. Measurement of mitochondrial membrane potential ($\Delta\Psi_m$)

The change in mitochondrial membrane potential of cell could be evaluated by the 5,5′,6,6′-tetrachloro-1,10,3,30-tetraethylbenzimidazol-carbocyanine iodide (JC-1) fluorescent probe (Mcelnea et al., 2011). After the cell treatment, HFF were incubated with JC-1 at 37 °C for 30 min, and then were centrifuged at 600*g* for 4 min. The collected cells were refloated and analyzed using a microplate reader after washing twice with PBS. The fluorescence intensity of JC-1 monomer was measured at excitation wavelength of 515 nm and emission wavelength of 529 nm. The fluorescence intensity of JC-1 polymer was measured at excitation wavelength of 585 nm and emission wavelength of 590 nm.

2.7. Reverse transcriptase polymerase chain reaction (RT-PCR)

The total mRNA of HFF was extracted by using Trizol after cell treatment. Then 20 μL of DNase I and 20 μL of 10 × PCR buffer were added into 60 μL of RNA to remove the pollution of genome. The complementary DNA (cDNA) was synthesized by reverse transcription reaction from purified mRNA. Real-time PCR was performed by use of the SYBR® Premix Ex Taq™ on the Hema9600 Gene amplifiers (Hema Medical Instrument Co. Ltd, Zhuhai, China). The forward and reverse primers used for PCR amplification of actin, elastin and collagen type-I gene are all listed in Table 1. The real-time PCR program was carried out with a following 1 cycle of initial denaturation at 95 °C for 30 s, 95 °C for 3 s, and 60 °C for 34 s through 40 cycles of PCR reaction. Finally, melting curve analysis was performed over a gradient extending from an annealing to a denaturation temperature (60–95 °C). The expression was calculated by using the relative standard curve method of quantification and reported as a fold change of gene

Table 1
Primer sequences used in this study.

Gene	Primer	Primer sequence (5′—3′)
actin	F	CACTGTCGAGTCGCGTCC
	R	CGCAGCGATATCGTCATCCA
Elastin	F	CACCACCCCACCTCTTTGTG
	R	CCAAAGAGCACACCAACAATCA
Collagen type I	F	GGGGCAAGACAGTCATCGAA
	R	GGGTGGAGGGAGTTTACACG

expression.

2.8. In vitro simulated GI digestion

A two-stage of digestion was used to simulate GI digestion. The pH of hydrolysate solution (10% w/w, dissolved in deionized water) was adjusted to 2.0 with 1 M HCl before pepsin (2% w/w) was added. The mixture was then incubated at 37 °C for 2 h before its pH was adjusted to 5.3 with 0.9 M $NaHCO_3$ and to 7.5 with 1 M NaOH. Then pancreatin (2% w/w) was added and the mixture was incubated at 37 °C for 4 h and finally heated in boiling water for 10 min to inactive the enzymes. All the samples were lyophilized and stored at −18 °C till use.

2.9. Caco-2 cell culture

Human colon cancer cells (Caco-2) were treated with DMEM containing penicillin (100 U/mL), streptomycin (100 μg/mL) and 10% FBS in a chamber of a 12-well Transwell plate (pore size 0.4 μm, chamber diameter 12 mm). Then the cells were incubated at 37 °C in a CO_2 incubator with 5% CO_2. The medium was changed every 2–3 days to allow the cells to grow for 24–28 days.

2.10. Transport of GLPY across Caco-2 cell monolayers

The integrity of the Caco-2 monolayers layers was evaluated by transepithelial electrical resistance (TEER) using a Millicell-ERS (Millipore Corporation, America). Only the Caco-2 monolayers with a TEER higher than 400 Ω cm^2 were used in the transport study. After washing with HBSS, Caco-2 monolayers were incubated with HBSS at 37 °C in a CO_2 incubator with 5% CO_2 for 2 h. Then 0.5 mL of GLPY (4 mM) dissolved in HBSS were added into the apical side and 1 mL of HBSS was added into the basolateral side. The cell culture plates were incubated at 37 °C for 2 h. Additionally, transport inhibitors cytochalasin D (0.5 μg/mL), Gly-Pro (10 mM), sodium azide (10 mM), and wortmannin (500 nM) were added to Caco-2 cell monolayers for 1 h before the transport study to identify the mechanism for the transepithelial absorption of GLPY. The absorbed permeates on the basolateral side were collected for further assays. The apparent permeability coefficient (P_{app}, cm/s) of peptide was measured as follow:

$$P_{app}(cm/s) = (dM_{R(t)}/d_t) / (A \times C_{d0})$$

where M_R is the amount of peptide in the receiver chamber (μM), t is the time (s), A is the area of the membrane (cm^2), and C_{d0} is the initial donor concentration (μM).

2.11. Peptide analysis by UPLC-ESI-QTOF-MS/MS

A Waters Acquity ultra-high performance liquid chromatography (UPLC, Waters Corporation, USA) system coupled to an IMPACT II Q-TOF mass spectrometer (Bruker Daltonics, Bremen, Germany) was used for identifying elastin peptides. The mass spectrometer was equipped with an electrospray ionization (ESI) source used in the positive ion mode. The samples were automatically injected to an HSS T3 column (2.1 mm × 50 mm, 1.8 μm, Waters Corporation, USA) and eluted with solvent A (H_2O containing 0.1% methanoic acid) and B (Acetonitrile). A flow rate of 0.2 μL/min was used with the following gradient: 5% solvent B at 1 min, increasing to 50% solvent B at 4 min, and then decreasing to 5% solvent B at 5 min, and finally maintained at 5% solvent B until 6 min. Mass range of 50–1000 and 50–1000 were scanned for the MS and MS/MS procedures, respectively. Interpretation of MS/MS spectra was performed using the Mascot software (Matrix Sciences, London, UK). For quantification, the peak area was compared with an external standard calibration curve obtained using synthetic peptides.

2.12. Statistical analysis

At least two independent trials were performed for each type of experiment. Each analysis was conducted in triplicate, and the data were presented as mean ± standard deviation. The results obtained were subjected to one-way analysis of variance (ANOVA). Duncan's new multiple range test was performed to determine the significant difference between samples at the 95% confidence interval using SPSS 19.0 software (SPSS Inc, Chicago, IL, USA).

3. Result and discussion

3.1. Effects of GLPY and GPGGVGAL on intracellular ROS production and SOD activity

In our previous study, the inhibitory effects of GLPY and GPGGVGAL on apoptosis of HFF induced by UV were evaluated (Liu et al., 2018). As shows in Fig. 1S, the cell viability of fibroblasts after exposure to UV irradiation for 24 h significantly ($p < 0.01$) reduced to 40.55% compared with the UV(-) group, and treatment with GLPY and GPGGVGAL could significantly ($p < 0.05$) inhibit the apoptosis of HFF in a dose-dependent manner at the concentrations ranged from 50 to 400 μM. Moreover, just slight increase ($p > 0.05$) in the cell viability was observed in UV-damaged fibroblasts treated with GLPY and GPGGVGAL at the concentration of 200 μM compare to 400 μM. Therefore, the protective effects of GLPY and GPGGVGAL at the concentration of 200 μM on UV-damaged fibroblasts were further investigated.

According to Fig. 1, the intracellular ROS production of UV-damaged HFF significantly ($p < 0.05$) increased to 117% of the control group. However, GLPY and GPGGVGAL could effectively reduce intracellular ROS to 105.82% and 104.25%, respectively. Additionally, the activity of antioxidase (i.e., SOD) was in negative correlation to the levels of intracellular ROS. The activity of SOD in UV-damaged HFF decreased from 86.16 U/mg to 66.76 U/mg, while the activities of SOD in HFF increased significantly after treatment with GLPY or GPGGVGAL.

Evidently, over-production of ROS (Fisher et al., 2002) and decrease of antioxidase activity in excessive UV-damaged cells (Mcardle et al., 2002) could lead to protein oxidation, DNA damage and mitochondrial dysfunction, and finally result in HFF apoptosis (Rinnerthaler, Bischof, Streubel, Trost, & Richter, 2015). The present results exhibited that GLPY and GPGGVGAL treatment could alleviate oxidative stress by increasing SOD activity and reducing ROS production. It could be a reason for the decrease in apoptosis of HFF treated with GLPY and GPGGVGAL (Liu et al., 2018).

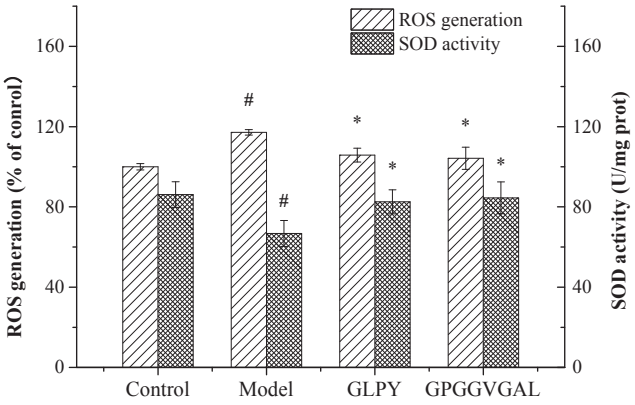

Fig. 1. Effects of GLPY and GPGGVGAL (200 μM) on the UV-induced intracellular ROS accumulation and SOD activity downregulation. The values are expressed as means ± SD from triplicate experiments. #, $p < 0.05$ versus control group; ∗, $p < 0.05$ versus model group.

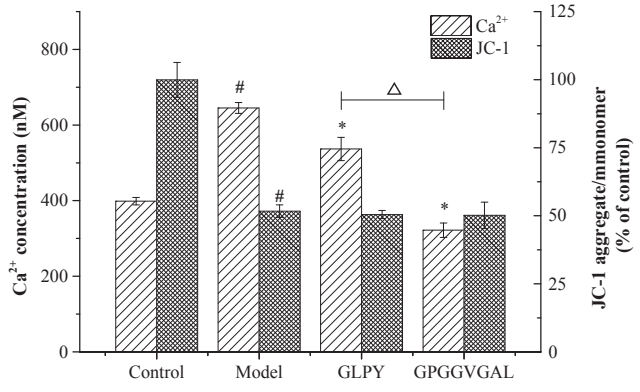

Fig. 2. Effects of GLPY and GPGGVGAL (200 μM) on the UV-induced Ca^{2+} influx and MMP loss. The values are expressed as means ± SD from triplicate experiments. #, $p < 0.05$ versus control group; ∗, $p < 0.05$ versus model group; △, significant differences between sample groups, $p < 0.05$.

3.2. Effects of GLPY and GPGGVGAL on intracellular Ca^{2+} concentration and mitochondrial membrane potential ($\Delta\Psi m$)

Accumulative ROS exhibited negative effect on mitochondria which led to Ca^{2+} influx (Zhang et al., 2015) and accumulative Ca^{2+} induced the generation of ROS (Sousa, Maciel, Vercesi, & Castilho, 2003). According to Fig. 2, the Ca^{2+} concentration in HFF after UV exposure dramatically increased to 161.79% of the UV(−) group. Both the two peptides could significantly ($p < 0.05$) decrease the Ca^{2+} concentration in HFF, and GPGGVGAL inhibited the increase of Ca^{2+} concentration (321.97 nM) more effectively while the Ca^{2+} concentration of HFF after treatment with GLPY just decreased to 536.63 nM.

Mitochondrial could intake large number of cytosolic Ca^{2+} and lead to the loss of mitochondrial membrane potential (Mcelnea et al., 2011). Hence the changes in Ca^{2+} concentration is usually accompanied by the changes in mitochondrial membrane potential. Obviously, a loss of mitochondrial membrane potential in UV damaged HFF is observed in Fig. 2. However, there is no significant ($p > 0.05$) difference between the model group and HFF treated with GLPY or GPGGVGAL.

The excessive cytosolic calcium concentration ($[Ca^{2+}]_i$), which has been demonstrated to have effects on mitochondria(Kadenbach, Arnold, Lee, & Hüttemann, 2004) and endoplasmic reticulum (Lamb et al., 2006), as well as activating Fas death receptor signaling (Ashkenazi & Dixit, 1998), is generally regarded as a signal for the activation of apoptosis. In the present study, GLPY and GPGGVGAL could inhibit the enhancement of Ca^{2+} concentration induced by UV irradiation, but showed no significant influence on mitochondrial membrane potential of HFF. It suggested that GLPY and GPGGVGAL might decrease Ca^{2+} concentration through other pathways (e.g. death receptor pathways) rather than the mitochondrial apoptosis pathway. As Choi, Lee, Park, Kim, and Lee (2008) pointed out, kalopanaxsaponin A isolated from *K. pictus* could promote the apoptosis of promonocytic leukemia U937 cells *via* caspase-8 activation induced by Ca^{2+} influx. Similar results were also reported by Zhao et al. (2017), in which both PAYCS and PAYCS could inhibit Ca^{2+} influx but had no effects on mitochondrial membrane potential.

3.3. Effects of GLPY and GPGGVGAL on concentration of elastin and collagen type-I

UV exposure could induce the collagenolysis and elastolysis in HFF. In order to investigate the inhibitory effect of peptides on the decrease of collagen and elastin in HFF, we measured the content of collagen type-I and elastin in HFF. As Fig. 3A displayed, elastin in HFF with UV exposure decreased to 91.69% of the control group. After treatment with GLPY, the elastin concentration significantly increased to 119.47% of the control group, and GPGGVGAL could also upregulate the levels of elastin. Likewise, UV exposure led to a remarkable decrease in collagen type-I (about 21.09%) while an obvious enhancement of collagen type-I in HFF was induced by both the two peptides, especially GLPY with 136.90% of the control group (Fig. 3B).

Collagen and elastin are the essential proteins in ECM to bestow skin with indispensable structure and mechanical properties. The degradation of ECM induced by UV would result in a decrease of cellular adhesion even anoikis (Chiarugi & Giannoni, 2008). The obtained results revealed that GLPY and GPGGVGAL could inhibit the loss of collagen type-I and elastin caused by UV irradiation, and similar inhibitory effect of peptides and natural products on UV-induced collagenolysis and elastolysis in HFF were widely reported (Hong et al., 2015; Kim et al., 2014; Shim, Kwon, & Hwang, 2008).

3.4. Effects of GLPY and GPGGVGAL on concentration of MMP-12 and MMP-1

According to Fig. 3C, UV exposure resulted in a dramatic enhancement of both MMP-1 and MMP-12 concentration (183.57% and 193.57% of the control group, respectively). The content of MMP-12 in HFF treated with GLPY significantly ($p < 0.05$) decreased to 174.21%, while GPGGVGAL exhibited less influence on MMP-12 concentration of HFF exposed to UV irradiation. Additionally, GLPY and GPGGVGAL could not ameliorate the upregulation of MMP-1 concentration which caused by UV exposure (Fig. 3D). Conversely, myristoyl tetrapeptide with the amino acid sequence GLFW was confirmed to suppresse the UV-induced expression of MMP-1(Kwon et al., 2016).

It is evident that MMP-1 and MMP-12, which are members of the matrix metalloproteinases (MMPs) family, are the key enzymes in degradation of collagen (Wang et al., 2016) and elastin (Van Doren, 2015). Excessive generation of ROS induced by UV could upregulate the mRNA expression of MMPs through activating the MAPK pathway (Yaar & Gilchrest, 2010). Therefore, the negative influence of GLPY on MMP-12 might result from the downregulation of MMP-12 by reducing the level of ROS (Fig. 1). Additionally, the MMP-12 inhibitory activity of GLPY, which has been demonstrated in our previous study (Liu et al., 2018), could also contribute to the lower content of MMP-12 in HFF. The low concentration activity of MMP-12 in HFF treated with GLPY would alleviate the degradation of elastin in HFF after UV treatment. Kim (2016) pointed out the similar results that garlic supplementation could protect hairless mice from UV-damage by regulating antioxidative activity and MMPs expression. Although obvious increase in collagen type-I was found in HFF treated with GLPY and GPGGVGAL (Fig. 3B), GLPY and GPGGVGAL could not inhibit the upregulation of MMP-1 concentration caused by UV exposure. It revealed that GLPY and GPGGVGAL might regulate the level of collagen type-I through reducing the levels of other MMPs. As Vayalil, Mittal, Hara, Elmets, and Katiyar (2004) reported, polyphenols from green tea could inhibit the degradation of ECM by inhibiting the expression of MMP-2, 3, 7 and 9. Furthermore, the regulation of the mRNA expression of collagen type-I and elastin might also contribute to the levels of collagen type-I and elastin.

3.5. Effects of GLPY and GPGGVGAL on mRNA expression of collagen type-I and elastin

UV radiation or free radicals could upregulate expression of elastin mRNA by activating elastin promoter, resulting in the deposition of abnormal elastic material (Bernstein, Brown, Schwartz, Kays, & Ksenzenko, 2010). Obviously, there was a dramatic change in mRNA expression of elastin in response to UV irradiation (Fig. 3E). The expression of elastin mRNA in HFF increased to 2.41 times of the control group due to the exposure on UV while both the two peptides obviously downregulated the mRNA expression of elastin. After treatment with GLPY and GPGGVGAL, the elastin mRNA expression of HFF reduced to

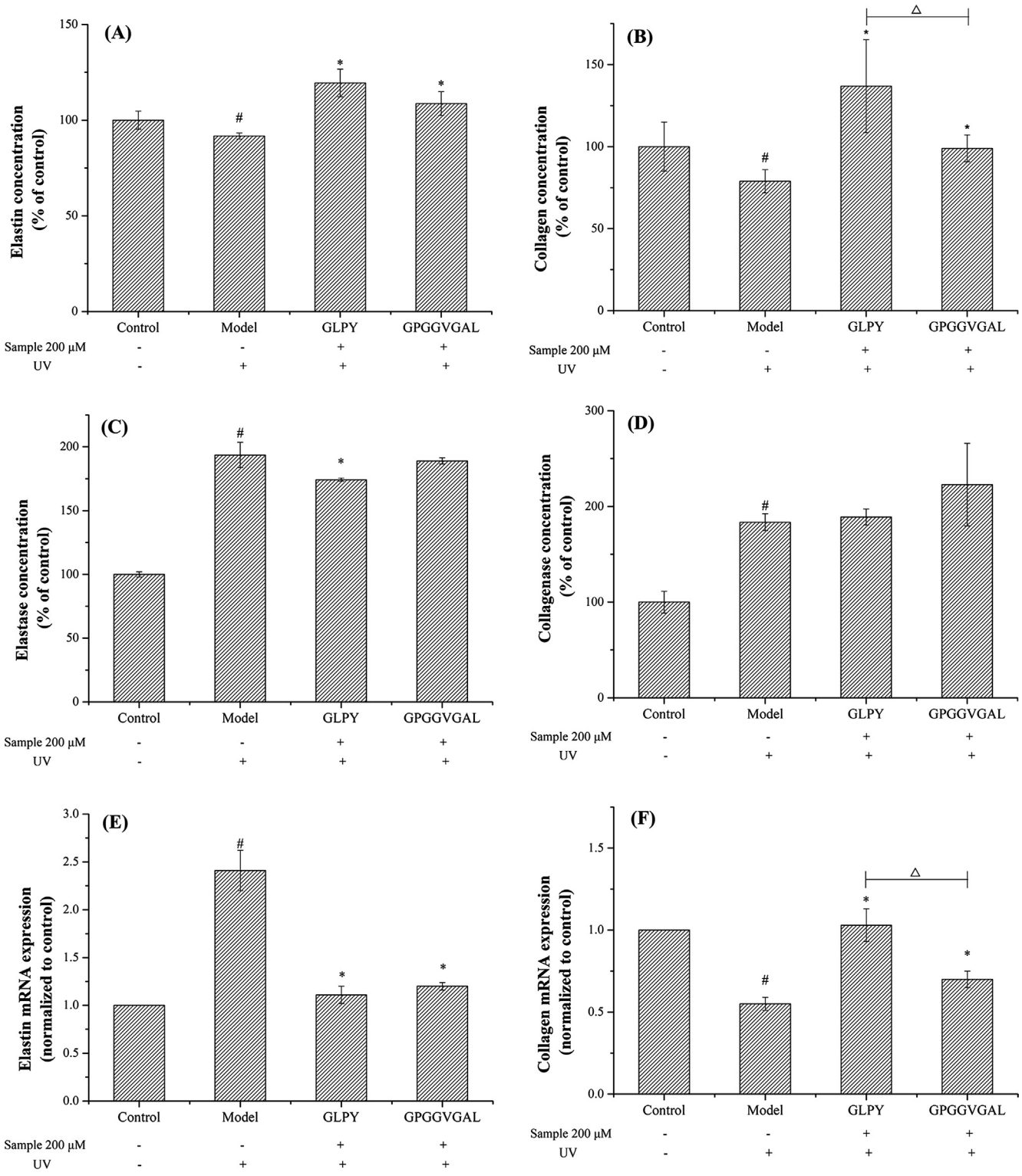

Fig. 3. Effects of GLPY and GPGGVGAL (200 μM) on the UV-induced upregulation of (A) elastin, (B) collagen type-I, (C) MMP-12, (D) MMP-1, and mRNA expression of (E) elastin and (F) collagen type-I. The values are expressed as means ± SD from triplicate experiments. #, $p < 0.05$ versus control group; ∗, $p < 0.05$ versus model group; △, significant differences between sample groups, $p < 0.05$.

1.11–1.20 times of HFF without UV exposure which was close to the normal level. Since ROS was considered to be responsible for the upregulation of elastin mRNA expression (Kawaguchi et al., 1997), the inhibitory effect of GLPY on ROS generation (Fig. 1) might be one reason for the regulation of the elastin mRNA expression. In addition, although a significant ($p < 0.05$) increase in elastin mRNA expression of HFF induced by UV exposure was observed, there was a minor decrease in elastin concentration. It might result from the upregulation of MMP-12 induced by UV which led to a remarkable degradation of elastin.

UV irradiation could impair the expression of transforming growth factor-β (TGF-β)/Smad (Quan, He, Kang, Voorhees, & Fisher, 2004),

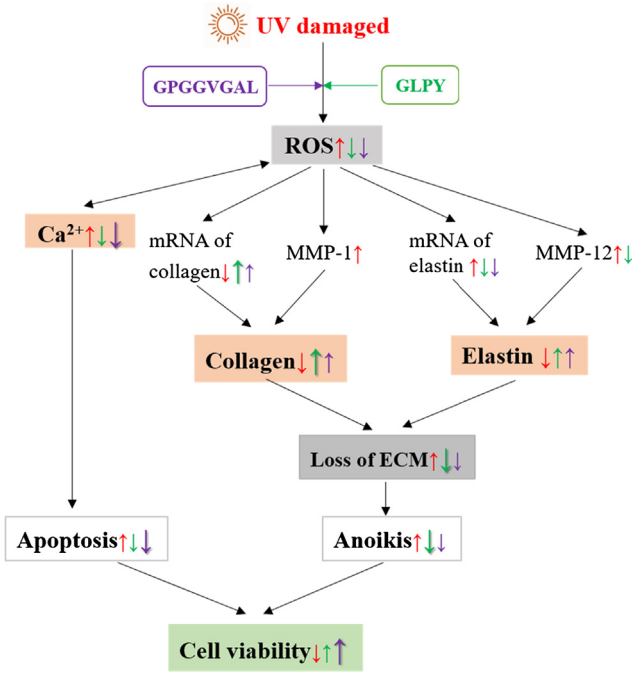

Fig. 4. The protective effect of GLPY and GPGGVGAL on the UV-damaged fibroblast.

which could lead to down-regulation of mRNA expression of collagen (Uchio, Graham, Dean, Rosenbaum, & Desmouliã Re, 2010). According to Fig. 3F, the level of collagen type-I mRNA expression in model group decreased to 55% compared to that in HFF without UV treatment, indicating that UV exposure would lead to a decrease in mRNA expression of collagen type-I. Fortunately, GLPY and GPGGVGAL could upregulate mRNA expression of collagen type-I, especially GLPY treatment resulted in a 0.87 times enhancement compared with the model group. It is possible that GLPY and GPGGVGAL inhibited the loss of collagen by upregulating the collagen type-I expression rather than reducing the MMP-1 concentration.

3.6. Proposed mechanism of the protective effects of GLPY and GPGGVGAL on the apoptosis of HFF

The proposed mechanism of the protective effects of GLPY and GPGGVGAL on HFF against UV damage was illustrated in Fig. 4. GLPY and GPGGVGAL could ameliorate the generation of ROS induced by UV to suppress the oxidative stress and also modulated the intracellular Ca^{2+} concentration. Since high level of Ca^{2+} could lead to apoptosis, the higher inhibition of Ca^{2+} influx showed by GPGGVGAL might be one reason for the higher cell viability of HFF treated with GPGGVGAL. Besides, the excessive ROS could activate MMPs and regulate mRNA expression of elastin and collagen, finally resulting in the loss of ECM which might be related to anoikis. The two peptides, especially GLPY could ameliorate the loss of collagen and elastin in fibroblasts exposed to UV possibly through three pathways. Firstly, GLPY could inhibit the degradation of elastin by reducing the level of MMP-12. Further, GLPY and GPGGVGAL could increase the synthesis of collagen by upregulating the mRNA expression of collagen type-I. Finally, GLPY and GPGGVGAL could effectively inhibit the activity of elastase (e.g. MMP-12) as showed in our previous study (Liu et al., 2018), and thus ameliorated elastolysis induced by UV exposure.

3.7. Degradation of GLPY and GPGGVGAL during in vitro GI digestion

It is widely accepted that peptides might be further digested before absorbing by gastrointestinal (GI) tract which would cause changes in the bioactivities of peptides (Lacroix et al., 2017; Wang, Liang, Chen, Xu, & Shi, 2014). In order to investigate the digestive stability of GLPY and GPGGVGAL, the two peptides were subjected to simulated GI digestion *in vitro*. The content of peptides was reflected by the peak area of the extracted ion chromatography (EIC) (Table 2). Obviously, although four fragments were found in the digesta of GLPY, the peak area of these fragments was below 8.00×10^5 counts, which was much lower than that of GLPY (3.27×10^6 counts). It indicated that most of GLPY were survived in the simulated digestion process. On the contrary, GPGGVGAL was completely digested into 6 peptide fragments. Notably, GPGGVGA was the main derivative peptides in the digesta of GPGGVGAL, followed by PGGVG. It suggested that GPGGVGAL was sensitive to the enzymes in GI tract and encapsulation of GPGGVGAL is required to remain intact during digestion and absorption processes. Similar results were reported by Ruiz et al. (2004), who found that some large peptides (e.g. KKYNVPQL) isolated from Manchego cheese were hydrolyzed to peptide fragments while smaller peptides such as LEIVPK and LPY remained intact after simulated GI digestion.

Table 2
Identification of GLPY, GPGGVGAL and their digesta after simulating gastrointestinal digestion *in vitro*.

Peptide Sequence		RT (min)	Prec. *m/z*	Area (counts)
GLPY				
After GI digestion	GLPY	3.6	449.2369	3,279,514
	PY	3.6	279.1320	788,658
	LPG	3.3	286.1743	193,975
	LPY	3.5	392.2158	23,475
	GL	4.8	189.1107	17,750
GPGGVGAL				
After GI digetsion	GPGGVGA	2.6	514.2611	10,913,010
	PGGVG	2.7	386.2017	951,350
	GPGGVG	2.6	443.2233	224,770
	GGVGA	2.5	360.1864	122,493
	PGGVGA	2.7	457.2394	114,311
	GVGA	2.5	303.1646	22,777

Many structure-activity studies have shown that the digestive sensibility of peptides or hydrolysates was determined by their molecular weight (Chen & Li, 2012), charge property (Ao & Li, 2013) and amino acid composition (Wang et al., 2016). The obtained results exhibited that the digestive stability of GLPY was stronger than that of GPGGVGAL. It might be due to the fact that the longer sequence of GPGGVGAL afforded more potential binding sites proposed between digestive enzyme and peptides. Furthermore, the peptide bond before proline (Pro) residue was rarely cleaved by pepsin (Keil, 1992). Hence the peak area of the EIC of GPGGVGA is the major peptide in GPGGVGAL digesta.

3.8. Apical-to-basolateral transport of GLPY

Caco-2 cells are used to investigate the absorption of peptides because of the morphological and functional characteristics similar to mature enterocytes (Sienkiewicz-Szłapka et al., 2009). In the present study, the transepithelial transport of GLPY, which was proved to resist GI digestion, was further studied. After incubation with Caco-2 cells, the concentration of GPLY reduced to 3.47 mM in apical layers (Table 3), indicating that about 6.50% of GLPY were further hydrolyzed by enzymes in brush boundary membrane. In addition, GL was not observed in apical layers while it was found in basolateral layers, suggesting that GL was released from GLPY and/or GLP by enzymes in Caco-2 cells during transepithelial transport. Furthermore, the concentration of GLPY in basolateral layers was 33.02 μM and its apparent permeability was 1.02×10^{-6} cm/s. It suggested that GLPY could be moderately (20–70%) absorbed *in vivo* (Yee, 1997).

Usually, peptides could cross intestinal epithelial cells *via* transporter PepT1, transcytosis or paracellular pathways mediated by tight junction protein (Shimizu & Son, 2010). It is widely reported that

Table 3
Identification of GLPY and its metabolites following incubation with Caco-2 monolayers.

	0 min (mM)	120 min	
		Apical (mM)	Basolateral (μM)
GLPY	4	3.47 ± 0.67	33.02 ± 1.52
GLP	–	√	√
LPY	–	√	√
PY	–	√	√
LP	–	√	√
GL	–	–	√

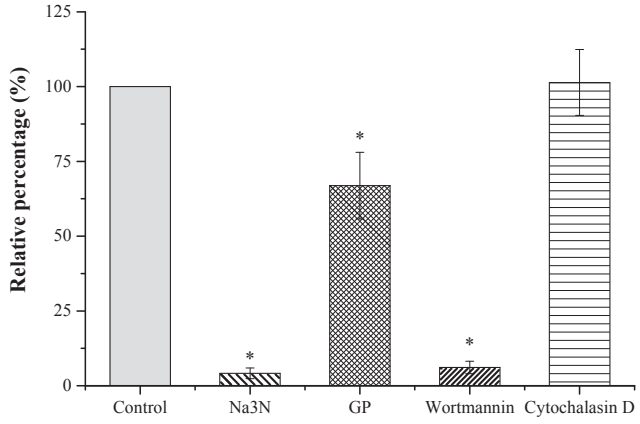

Fig. 5. Effects of Gly-Pro, cytochalasin D, wortmannin, and sodium azide on the transport of GLPY across the Caco-2 cell monolayers. The values are expressed as means ± SD from triplicate experiments. *, $p < 0.05$ versus control group.

wortmannin is an inhibitor of transcytosis, Na_3N has a negative effect on the release of ATP in cells, Cytochalasin D can expand cell junctions, while dipeptide GP can competitively bind to PepT1 to inhibit the transfer of oligopeptides (Contreras, Sancho, Recio, & Mills, 2012). Consequently, the transport mechanism of GLPY could be evaluated by adding selective inhibitors of transfer to Caco-2 monolayers. According to Fig. 5, after cytochalasin D loading on the apical side, no significant change was observed in the transport of GLPY while it dramatically decreased to 4.16% and 6.11% of the control in the presence of NaN_3 and wortmannin, respectively. It showed that GLPY could be absorbed *via* the intracellular transcytosis pathway which need a lot of ATP. Further, the addition of GP led to a 33.10% decrease of the transport of GLPY. It is obvious that part of GLPY was transferred by PepT1 across Caco-2 monolayers. In general, PepT1 plays an important role in the transport of dipeptides and tripeptides (Bolger et al., 1998), whereas larger peptides such as QIGLF (Ding et al., 2014), TNGIIR (Ding, Wang, Yu, Zhang, & Liu, 2016), YWDHNNPQIR (Xu et al., 2017) were permeated *via* the intracellular transcytosis pathway or paracellular pathways. Herein the tetrapeptide GLPY could transport into intestinal epithelial cells *via* both transporter PepT1 and transcytosis pathways.

4. Conclusion

In conclusion, GLPY and GPGGVGAL exhibited protective effects on HFF cells against UV-damage through inhibiting the upregulation of ROS, Ca^{2+} influx, collagenolysis and elastolysis. Specially, GPGGVGAL showed higher suppression on Ca^{2+} influx while GLPY displayed stronger inhibition of ECM (including collagen and elastin) degradation caused by downregulation of MMP-12 and upregulation of mRNA expression of collagen type-I. Further, GPGGVGAL was completely hydrolyzed during the GI digestion *in vitro*, whereas GLPY survived in GI tract and remained intact across Caco-2 monolayers *via* the intracellular transcytosis pathway. However, in order to further explore the protective effect of GLPY on photoaging skin *in vivo*, it is necessary to investigate whether the GPLY could reach *in vivo* target sites (e.g. fibroblasts) in an intact form and display its bioactivity.

Ethics statement

On behalf of, and having obtained permission from all the authors, I declare that:

a. The material has not been published in whole or in part elsewhere;
b. The paper is not currently being considered for publication elsewhere;
c. All authors have been personally and actively involved in substantive work leading to the report, and will hold themselves jointly and individually responsible for its content;
d. No clinical or animal studies were involved in this study

Declaration of Competing Interest

We declare that we have no financial and personal relationships with other people or organizations that can inappropriately influence our work, there is no professional or other personal interest of any nature or kind in any product, service and/or company that could be construed as influencing the position presented in, or the review of, the manuscript entitled.

Acknowledgements

This work was supported by the National Key Research and Development Program of China (No. 2017YFD0400201), the National Postdoctoral Program for Innovative Talents of China (No. BX201700081) and the Natural Science Foundation of Guangxi (No. 2016GXNSFEA380003).

Appendix A. Supplementary material

Supplementary data to this article can be found online at https://doi.org/10.1016/j.jff.2019.103487.

References

Ao, J., & Li, B. (2013). Stability and antioxidative activities of casein peptide fractions during simulated gastrointestinal digestion *in vitro*: Charge properties of peptides affect digestive stability. *Food Research International, 52*, 334–341.
Ashkenazi, A., & Dixit, V. M. (1998). Death receptors: Signaling and modulation. *Science, 281*, 1305–1308.
Bernstein, E. F., Brown, D. B., Schwartz, M. D., Kays, K., & Ksenzenko, S. M. (2010). The polyhydroxy acid gluconolactone protects against ultraviolet radiation in an in vitro model of cutaneous photoaging. *Dermatologic Surgery, 30*, 189–196.
Bolger, M. B., Haworth, I. S., Yeung, A. K., Ann, D., Grafenstein, H. V., Hamm-Alvarez, S., ... Wu, S. (1998). Structure, function, and molecular modeling approaches to the study of the intestinal dipeptide transporter PepT1. *Journal of Pharmaceutical Sciences, 87*, 1286–1291.
Chen, M., & Li, B. (2012). The effect of molecular weights on the survivability of casein-derived antioxidant peptides after the simulated gastrointestinal digestion. *Innovative Food Science & Emerging Technologies, 16*, 341–348.
Chiarugi, P., & Giannoni, E. (2008). Anoikis: A necessary death program for anchorage-dependent cells. *Biochemical Pharmacology, 76*, 1352–1364.
Choi, J., Lee, H., Park, H., Kim, S., & Lee, K. (2008). Kalopanaxsaponin A induces apoptosis in human leukemia U937 cells through extracellular Ca^{2+} influx and caspase-8 dependent pathways. *Food and Chemical Toxicology, 46*, 3486–3492.
Contreras, M. D. M., Sancho, A. I., Recio, I., & Mills, C. (2012). Absorption of casein antihypertensive peptides through an *in vitro* model of intestinal epithelium. *Food Digestion, 3*, 16–24.
Ding, L., Wang, L., Yu, Z., Zhang, T., & Liu, J. (2016). Digestion and absorption of an egg white ACE-inhibitory peptide in human intestinal Caco-2 cell monolayers. *International Journal of Food Sciences and Nutrition, 67*, 111–116.
Ding, L., Zhang, Y., Jiang, Y., Wang, L., Liu, B., & Liu, J. (2014). Transport of egg white ACE-inhibitory peptide, Gln-Ile-Gly-Leu-Phe, in human intestinal Caco-2 cell monolayers with cytoprotective effect. *Journal of Agricultural and Food Chemistry, 62*, 3177–3182.
Fisher, G. J., Datta, S., Wang, Z., Li, X. Y., Quan, T., Chung, J. H., ... Voorhees, J. J. (2000). c-Jun-dependent inhibition of cutaneous procollagen transcription following

ultraviolet irradiation is reversed by all-trans retinoic acid. *Journal of Clinical Investigation, 106*, 663–670.
Fisher, G. J., Kang, S., Varani, J., Batacsorgo, Z., Wan, Y., Datta, S., & Voorhees, J. J. (2002). Mechanisms of photoaging and chronological skin aging. *Archives of Dermatology, 138*, 1462–1470.
Helfrich, Y. R., Sachs, D. L., & Voorhees, J. J. (2008). Overview of skin aging and photoaging. *Dermatology Nursing, 20*, 177–183 quiz 184.
Hong, Y., Lee, H. Y., Jung, B. J., Jang, S., Chung, D. K., & Kim, H. (2015). Lipoteichoic acid isolated from *Lactobacillus plantarum* down-regulates UV-induced MMP-1 expression and up-regulates type I procollagen through the inhibition of reactive oxygen species generation. *Molecular Immunology, 67*, 248–255.
Kadenbach, B., Arnold, S., Lee, I., & Hüttemann, M. (2004). The possible role of cytochrome c oxidase in stress-induced apoptosis and degenerative diseases. *BBA - Bioenergetics, 1655*, 400–408.
Kawaguchi, Y., Tanaka, H., Okada, T., Konishi, H., Takahashi, M., Ito, M., & Asai, J. (1997). Effect of reactive oxygen species on the elastin mRNA expression in cultured human dermal fibroblasts. *Free Radical Biology and Medicine, 23*, 162–165.
Keil, B. (1992). *Specificity of proteolysis.* Berlin Heidelberg: Springer201-201.
Kim, D., Kim, H., Kim, H., Jung, H., Yu, J., Lee, E., ... An, B. (2014). CopA3 peptide prevents ultraviolet-induced inhibition of type-I procollagen and induction of matrix metalloproteinase-1 in human skin fibroblasts. *Molecules, 19*, 6407–6414.
Kim, H. K. (2016). Garlic supplementation ameliorates UV-induced photoaging in hairless mice by regulating antioxidative activity and MMPs expression. *Molecules,* 21.
Kwon, H., Ahn, E., Kim, S., Kang, Y., Kim, M. O., Jin, B. S., & Park, S. (2016). Inhibition of UV-induced matrix metabolism by a myristoyl tetrapeptide. *Cell Biology International, 40*, 257–268.
Lacroix, I., Chen, X. M., Kitts, D. D., & Li-Chan, E. (2017). Investigation into the bioavailability of milk protein-derived peptides with dipeptidyl-peptidase IV inhibitory activity using Caco-2 cell monolayers. *Food Function, 8*, 701–709.
Lamb, H. K., Mee, C., Xu, W., Liu, L., Blond, S., Cooper, A., ... Hawkins, A. R. (2006). The affinity of a major Ca^{2+} binding site on GRP78 is differentially enhanced by ADP and ATP. *Journal of Biological Chemistry, 281*, 8796–8805.
Liu, Y., Su, G., Zhou, F., Zhang, J., Zheng, L., & Zhao, M. (2018). Protective effect of bovine elastin peptides against photoaging in mice and identification of novel anti-photoaging peptides. *Journal of Agricultural and Food Chemistry, 66*, 10760–10768.
Mcardle, F., Rhodes, L. E., Parslew, R., Jack, C. I., Friedmann, P. S., & Jackson, M. J. (2002). UVR-induced oxidative stress in human skin *in vivo*: Effects of oral vitamin C supplementation. *Free Radical Biology & Medicine, 33*, 1355–1362.
Mcelnea, E. M., Quill, B., Docherty, N. G., Irnaten, M., Siah, W. F., Clark, A. F., O Brien, C. J., & Wallace, D. M. (2011). Oxidative stress, mitochondrial dysfunction and calcium overload in human lamina cribrosa cells from glaucoma donors. *Molecular Vision, 17*, 1182–1191.
Muller, F. L., Lustgarten, M. S., Youngmok, J., Arlan, R., & Holly, V. R. (2007). Trends in oxidative aging theories. *Free Radical Biology & Medicine, 43*, 477–503.
Park, B., Hwang, E., Seo, S. A., Zhang, M., Park, S., & Yi, T. (2017). Dietary *Rosa damascena* protects against UVB-induced skin aging by improving collagen synthesis via MMPs reduction through alterations of c-Jun and c-*Fos* and TGF-beta 1 stimulation mediated smad2/3 and smad7. *Journal of Functional Foods, 36*, 480–489.
Quan, T., He, T., Kang, S., Voorhees, J. J., & Fisher, G. J. (2004). Solar ultraviolet irradiation reduces collagen in photoaged human skin by blocking transforming growth factor-beta type II receptor/Smad signaling. *American Journal of Pathology, 165*, 741–751.
Rinnerthaler, M., Bischof, J., Streubel, M. K., Trost, A., & Richter, K. (2015). Oxidative stress in aging human skin. *Biomolecules, 5*, 545–589.
Ruiz, J.Á. G., Ramos, M., & Recio, I. (2004). Angiotensin converting enzyme-inhibitory activity of peptides isolated from Manchego cheese. Stability under simulated gastrointestinal digestion. *International Dairy Journal, 14*, 1075–1080.
Ryu, B., Qian, Z. J., & Kim, S. K. (2010). SHP-1, a novel peptide isolated from seahorse inhibits collagen release through the suppression of collagenases 1 and 3, nitric oxide products regulated by NF-kappaB/p38 kinase. *Peptides, 31*, 79–87.
Schwartz, E., Cruickshank, F. A., Christensen, C. C., Perlish, J. S., & Lebwohl, M. (2010). Collagen alterations in chronically sun-damaged human skin. *Photochemistry & Photobiology, 58*, 841–844.
Shim, J., Kwon, Y., & Hwang, J. (2008). The effects of panduratin A isolated from *kaempferia pandurata* on the expression of matrix metalloproteinase-1 and type-1 procollagen in human skin fibroblasts. *Planta Medica, 74*, 239–244.
Shimizu, M., & Son, D. O. (2010). Food-derived peptides and intestinal functions. *Current Pharmaceutical Design, 13*, 885–895.
Sienkiewicz-Szłapka, E., Jarmołowska, B., Krawczuk, S., Kostyra, E., Kostyra, H., & Bielikowicz, K. (2009). Transport of bovine milk-derived opioid peptides across a Caco-2 monolayer. *International Dairy Journal, 19*, 252–257.
Sousa, S. C., Maciel, E. N., Vercesi, A. E., & Castilho, R. F. (2003). Ca^{2+}-induced oxidative stress in brain mitochondria treated with the respiratory chain inhibitor rotenone. *Febs Letters, 543*, 179–183.
Sun, L., Liu, Q., Fan, J., Li, X., & Zhuang, Y. (2018). Purification and characterization of peptides inhibiting MMP-1 activity with C terminate of Gly-Leu from simulated gastrointestinal digestion hydrolysates of tilapia (*Oreochromis niloticus*) skin gelatin. *Journal of Agricultural and Food Chemistry, 66*, 593–601.
Uchio, K., Graham, M., Dean, N. M., Rosenbaum, J., & Desmouliã Re, A. (2010). Down-regulation of connective tissue growth factor and type I collagen mRNA expression by connective tissue growth factor antisense oligonucleotide during experimental liver fibrosis. *Wound Repair & Regeneration, 12*, 60–66.
Van Doren, S. R. (2015). Matrix metalloproteinase interactions with collagen and elastin. *Matrix Biology, 44–46*, 224–231.
Vayalil, P. K., Mittal, A., Hara, Y., Elmets, C. A., & Katiyar, S. K. (2004). Green tea polyphenols prevent ultraviolet light-induced oxidative damage and matrix metalloproteinases expression in mouse skin. *Journal of Investigative Dermatology, 122*, 1480–1487.
Wang, C., Wang, B., & Li, B. (2016). Bioavailability of peptides from casein hydrolysate *in vitro*: Amino acid compositions of peptides affect the antioxidant efficacy and resistance to intestinal peptidases. *Food Research International, 81*, 188–196.
Wang, L., Liang, Q., Chen, Q., Xu, J., & Shi, Z. (2014). Hydrolysis kinetics and radical-scavenging activity of gelatin under simulated gastrointestinal digestion. *Food Chemistry, 163*, 1–5.
Xu, F., Wang, L., Ju, X., Zhang, J., Yin, S., Shi, J., ... Yuan, Q. (2017). Transepithelial transport of YWDHNNPQIR and its metabolic fate with cytoprotection against oxidative stress in human intestinal Caco-2 cells. *Journal of Agricultural and Food Chemistry, 65*, 2056–2065.
Yaar, M., & Gilchrest, B. A. (2010). Photoageing: Mechanism, prevention and therapy. *British Journal of Dermatology, 157*, 874–887.
Yang, Y., He, H., Wang, F., Ju, X., Yuan, J., Wang, L., ... He, R. (2017). Transport of angiotensin converting enzyme and renin dual inhibitory peptides LY, RALP and TF across Caco-2 cell monolayers. *Journal of Functional Foods, 35*, 303–314.
Yee, S. (1997). In vitro permeability across Caco-2 cells (colonic) can predict in vivo (small intestinal) absorption in man–fact or myth. *Pharmaceutical Research, 14*, 763–766.
Zhang, Y., Han, L., Qi, W., Cheng, D., Ma, X., Hou, L., ... Wang, C. (2015). Eicosapentaenoic acid (EPA) induced apoptosis in HepG2 cells through ROS–Ca^{2+}–JNK mitochondrial pathways. *Biochemical and Biophysical Research Communications, 456*, 926–932.
Zhao, T., Su, G., Wang, S., Zhang, Q., Zhang, J., Zheng, L., ... Zhao, M. (2017). Neuroprotective effects of acetylcholinesterase inhibitory peptides from anchovy (*Coilia mystus*) against glutamate-induced toxicity in PC12 cells. *Journal of Agricultural and Food Chemistry, 65*, 11192–11201.